

# Simulation of the Initiated Addition of Hydrocarbon Free Radicals and Hydrogen Atoms to Oxygen via a Nonbranched Chain Mechanism

M. M. Silaev

Moscow State University, Vorob'evy gory, Moscow, 119992 Russia

e-mail: mmsilaev@rc.chem.msu.ru

Received February 1, 2007

**Abstract**—A reaction scheme is suggested for the nonbranched-chain free-radical oxidation of hydrocarbons. The scheme includes the formation of a low-reactivity radical  $RO_4^\bullet$  (e.g.,  $o\text{-CH}_3\text{C}_6\text{H}_4\text{CH}_2\text{O}_4^\bullet$ ) not participating in further chain propagation. This reaction can effectively compete with reactions of chain propagation via the reactive hydrocarbon radical  $R^\bullet$  and, as the oxygen concentration in the reaction mixture is increased, begins to inhibit the chain process. The kinetic equation derived from the reaction scheme using the quasi-steady-state treatment provide a description for the nonmonotonic (peaking) dependence of the rate of the chain formation of molecular oxidation products on the oxygen concentration. The energetics of key radical–molecular reactions is considered, and the reaction scheme suggested is applied to the nonbranched-chain hydrogen oxidation involving the low-reactivity radical  $HO_4^\bullet$ .

DOI: 10.1134/S0040579507060073

In recent publications [1, 2], we considered the kinetics of the nonbranched-chain addition of saturated free radicals at the C=C and C=O double bonds of alkene and formaldehyde molecules, respectively. The chain propagation steps of the kinetic schemes suggested for these processes include reactions parallel to, or competing with, chain propagation through a reactive free radical. Here, the same approach is taken to analyze the addition of hydrocarbon free radicals (including unsaturated ones) and hydrogen atoms to the oxygen molecule.

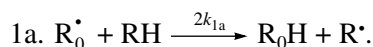
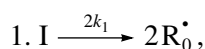
The addition of a free radical or an atom to one of the two multiply bonded atoms of the oxygen molecule yields a peroxy free radical and thus initiates oxidation, which is the basic process of chemical evolution. The peroxy free radical then abstracts the most labile atom from a molecule of the compound being oxidized or decomposes to turn into a molecule of an oxidation product. The only reaction that can compete with these two reactions at the chain propagation stage is the addition of the peroxy radical to the oxygen molecule (provided that the oxygen concentration is sufficiently high). This reaction yields a secondary, tetraoxyalkyl, 1 : 2 adduct radical, which is the heaviest and the largest among the reactants. It is less reactive than the primary, 1 : 1 peroxy adduct radical and, as a consequence, does not participate in further chain propagation. At moderate temperatures, the reaction proceeds via a nonbranched chain mechanism.

## ADDITION OF HYDROCARBON FREE RADICALS

Usually, the convex curve of the hydrocarbon (RH) autooxidation rate as a function of the partial pressure of oxygen ascends up to some limit and then flattens out [3]. When this is the case, the oxidation kinetics is satisfactorily described in terms of the conventional reaction scheme [3–8], which involves two types of free radicals. These are the hydrocarbon radical  $R^\bullet$ , which adds to an oxygen molecule and is a chain carrier (addend), and the addition product  $RO_2^\bullet$  (1 : 1 adduct). However, the existing mechanisms are inapplicable to the cases in which the rate of initiated oxidation as a function of the oxygen concentration has a maximum (Figs. 1, 2) [9, 10]. Such dependences can be described in terms of the earlier reported competition kinetics of free-radical chain addition [1, 2], whose reaction scheme involves not only the above two types of free radicals, but also an  $RO_4^\bullet$  radical (1 : 2 adduct) inhibiting the chain process.

### Reaction Scheme

Chain initiation:



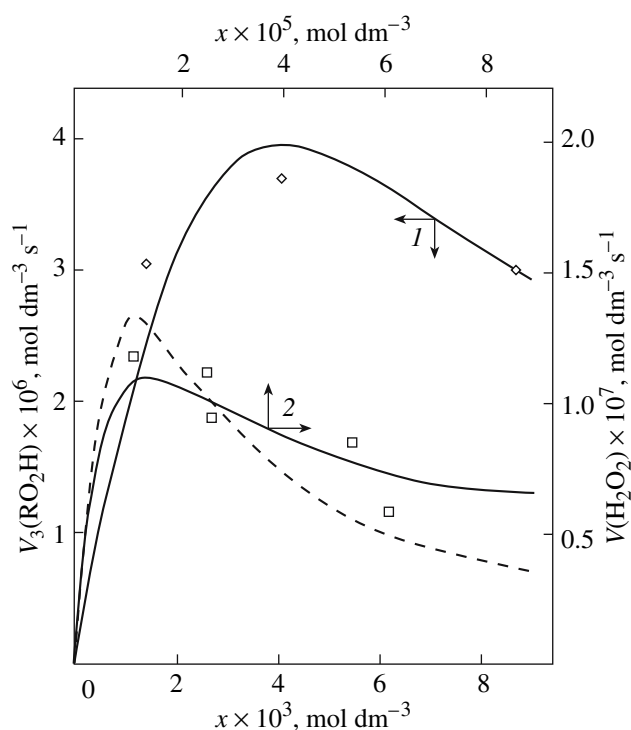
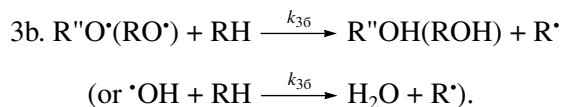
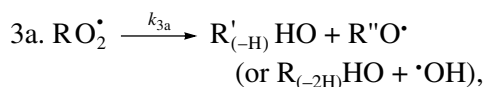
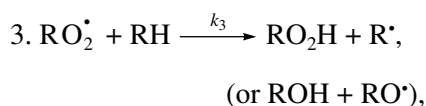
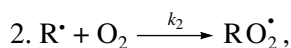


**Fig. 1.** (1) Reconstruction of the functional dependence of the 2-methylbenzyl hydroperoxide formation rate  $V_3(\text{RO}_2\text{H})$  on the initial dissolved-oxygen concentration  $x$  from empirical data (1) for the *o*-xylene–oxygen system [9] using Eq. (1a) with  $\beta = 0$  (model optimization with respect to the parameter  $\alpha$ ); the standard deviation of the fitted function is  $S_Y = 5.37 \times 10^{-7}$ . (2) Reconstruction of the functional dependence of the total hydrogen peroxide formation rate  $V_{3,7}(\text{H}_2\text{O}_2)$  on the initial dissolved-oxygen concentration  $x$  from empirical data (2) for the  $\gamma$ -radiolysis of water saturated with hydrogen and containing various amounts oxygen [34] using Eqs. (1a) and (5) with  $\beta = 0$  (model optimization with respect to the parameter  $\alpha$ );  $S_Y = 1.13 \times 10^{-8}$ . The dashed curve illustrates the description of the rate  $V_3(\text{H}_2\text{O}_2)$  as a function of the initial oxygen concentration  $x$  based on Eq. (1a) (model optimization with respect to  $\alpha$ ) and the experimental data of curve 2 ( $S_Y = 1.73 \times 10^{-8}$ ).

Chain propagation:



Inhibition:

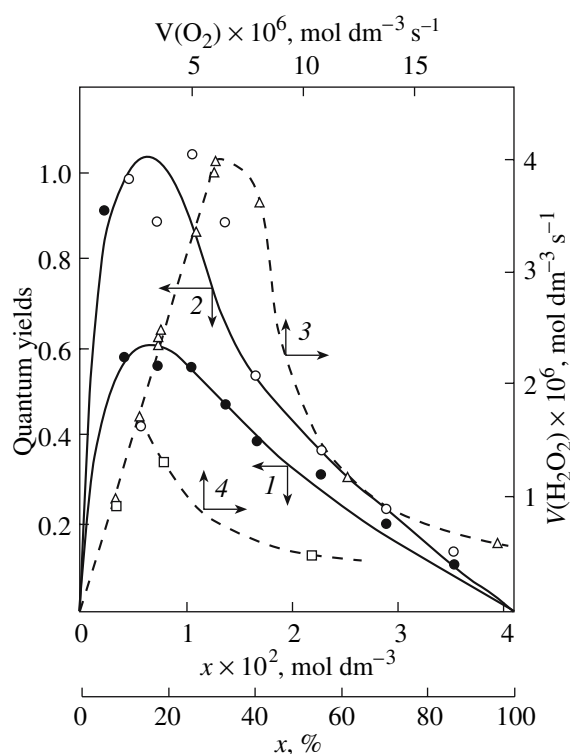
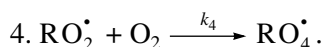
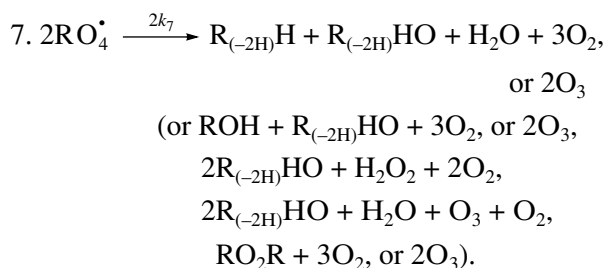
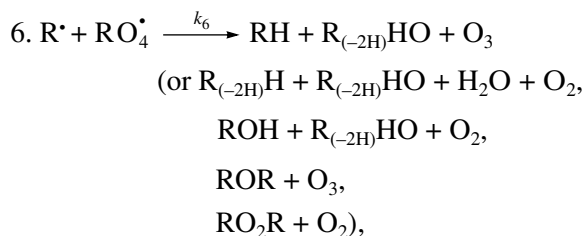
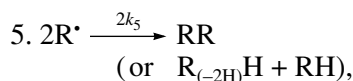


**Fig. 2.** Quantum yields of (1) hydrogen peroxide and (2) water resulting from the photochemical oxidation of hydrogen in the hydrogen–oxygen system as a function of the initial oxygen concentration  $x$  (light wavelengths of 171.9–172.5 nm, total pressure of  $10^5$  Pa, room temperature [32]). Hydrogen peroxide formation rate  $V(\text{H}_2\text{O}_2)$  as a function of the rate  $V(\text{O}_2)$  at which molecular oxygen is passed through a discharge tube filled with (3) atomic and (4) molecular hydrogen; atomic hydrogen was obtained from molecular hydrogen in the discharge tube before the measurements (total pressure of 25–77 Pa, temperature of 77 K [10]). The symbols represent experimental data.

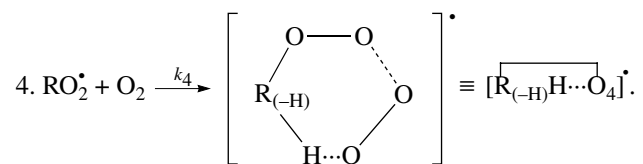
Chain termination:



The chain initiation and evolution stages of this scheme include the pairs of consecutive reactions 1–1a, 2–3, and 3a–3b; the pairs of parallel (competing) reactions 3–3a, 3–4, and 3a–4; and the pair of consecutive–parallel reactions 2–4. The only difference between the kinetic model of oxidation defined by this scheme and the kinetic model of the chain addition of 1-hydroxy-alkyl radicals to the free (unsolvated) form of formaldehyde in nonmethanolic alcohol–formaldehyde systems [2, 11, 12] is that reaction 4 in the former yields no molecular 1 : 1 adduct.

The decomposition of the initiator I in reaction 1 yields a reactive  $R_0^\bullet$  radical, which is converted into the ultimate product  $R_0H$  according to reaction 1a, generating an alkyl radical  $R^\bullet$ , which participates in chain propagation. In reaction 2, the addition of the free radical  $R^\bullet$  to the oxygen molecule yields a reactive alkylperoxy 1 : 1 radical adduct  $RO_2^\bullet$  [8], which possesses increased energy owing to the energy released upon the conversion of the  $O=O$  bond into the ordinary bond  $RO-O^\bullet$  (for addition in the gas phase under standard conditions, this energy is 115–130  $\text{kJ mol}^{-1}$  for the  $C_1$ – $C_4$  alkyl radicals [3, 13, 14] and 73  $\text{kJ mol}^{-1}$  for the allyl radical [13]). Because of this, the radical adduct can decompose (reaction 3a) or react with some neighbor molecule (reaction 3 or 4) on the spot, without diffusing in the solution and, accordingly, without entering into any chain termination reaction. In reaction 3, the interaction between the radical adduct  $RO_2^\bullet$  and the hydrocarbon molecule  $RH$  yields, via a chain mechanism, the alkyl hydroperoxide  $RO_2H$  (this reaction regenerates the chain carrier  $R^\bullet$  and, under certain conditions, can be viewed as a reversible reaction [4]) or the alcohol  $ROH$  (this is followed by the regeneration of  $R^\bullet$  via reaction 3b). The latter (alternative) pathway of reaction 3 consists of four steps, namely, the breaking of old bonds and the formation of two new bonds in the reacting structures. In reaction 3a, the isomerization and decomposition of the alkylperoxy radical adduct  $RO_2^\bullet$  with  $O-O$  and  $C-O$  or  $C-H$  bond breaking take place [3, 6], yielding the carbonyl compound  $R'_{(-H)}HO$  or  $R_{(-2H)}HO$ . Reaction 3b produces the alcohol  $R''OH$  or water and regenerates the free radical  $R^\bullet$  (here,  $R'$  and  $R''$  are radicals having a smaller number of carbon atoms than  $R$ ). As follows from the above scheme of the process, consecutive reactions 3a and 3b (whose rates are equal within the quasi-steady-state treatment), in which the highly reactive fragment radical oxyl  $R''O^\bullet$  (or  $^\bullet OH$ ) forms and then disappears, respectively, can be represented as the single, combined bimolecular reaction 3a,b occurring in a “cage” of solvent molecules. Likewise, the alternative (parenthesized) pathways of reactions 3 and 3b, which involve the alkoxy radical  $RO^\bullet$ , can formally be treated as having equal

rates. For simple alkyl  $C_1$ – $C_4$  radicals  $R$ , the pathway of reaction 3 leading to the alkyl hydroperoxide  $RO_2H$  is endothermic ( $\Delta H_{298}^\circ = 30$ – $80 \text{ kJ mol}^{-1}$ ) and the alternative pathway yielding the alcohol  $ROH$  is exothermic ( $\Delta H_{298}^\circ = -120$  to  $-190 \text{ kJ mol}^{-1}$ ), while the parallel reaction 3a, which yields a carbonyl compound and the alkoxy radical  $R''O^\bullet$  or the hydroxyl radical  $^\bullet OH$ , is exothermic in both cases ( $\Delta H_{298}^\circ = -80$  to  $-130 \text{ kJ mol}^{-1}$ ), as also is reaction 3b ( $\Delta H_{298}^\circ = -10$  to  $-120 \text{ kJ mol}^{-1}$ ), consecutive to reaction 3a, according to gas-phase thermochemical data [4, 14, 15]. In reaction 4, which is competing with (parallel to) reactions 3 and 3a (chain propagation through the reactive radical  $R^\bullet$ ), the resulting low-reactivity radical<sup>1</sup> that does not participate in further chain propagation and inhibits the chain process is supposed to be the alkyltetraoxy 1 : 2 radical adduct  $RO_4^{\bullet 2}$ , which has the largest weight and size. This radical is possibly stabilized by a weak intramolecular  $H\cdots O$  hydrogen bond [22] shaping it into a six-membered cyclic structure<sup>3</sup> (seven-membered cyclic structure in the case of aromatic and certain branched acyclic hydrocarbons) [24, 25]:



Reaction 4 in the case of the methylperoxy radical  $\text{CH}_3\text{O}_2^\bullet$  adding to the oxygen molecule to yield the

<sup>1</sup> It was hypothesized that the intermediate complex  $[\text{ROO}^\bullet \cdots \text{O}_2]$  can form reversibly in the *o*-xylene–oxygen system as the oxygen concentration is increased [9]. This complex is similar to the complex that is assumed here to be formed by the alkylperoxy 1 : 1 radical adduct and an unsaturated hydrocarbon— $[\text{ROO}^\bullet \cdots (\pi\text{-bond})\text{RH}]$ . The electronic structure of  $\pi$  complexes was considered by Buchachenko [16].

<sup>2</sup> Thermochemical data are available for some polyoxy free radicals (from which the enthalpy of formation of the methyltetraoxy radical without regard for the energy of the possible intramolecular hydrogen bond  $H\cdots O$  is  $\Delta H_{f298}^\circ(\text{CH}_3\text{O}_4^\bullet) = 121.3 \pm 15.3 \text{ kJ mol}^{-1}$ ) and polyoxides ( $\Delta H_{f298}^\circ(\text{CH}_3\text{O}_4\text{H}) = -21.0 \pm 9 \text{ kJ mol}^{-1}$ ) [17]. These data were obtained using the additive group approach. Some physicochemical and geometric parameters were calculated for the molecule of methyl hydroxytetraoxide as a model compound [18–20]. The IR spectra of dimethyl tetraoxide with isotopically labeled groups in  $\text{Ar-O}_2$  matrices were also reported [21]. For reliable determination of the number of oxygen atoms in an oxygen-containing species, it is necessary to use IR and ESR spectroscopy in combination with the isotope tracer method [21].

<sup>3</sup> An  $\overline{\text{R}_{(-H)}\text{H} \cdots \text{O}(\text{R})\text{O}_3}$  ring consisting of the same six atoms (C, H, and 4O), presumably with a hydrogen bond [3], also forms in the transition state of the dimerization of primary and secondary alkylperoxy radicals ( $RO_2^\bullet$ ) via the Russell mechanism [5, 23].

methyltetraoxy radical  $\text{CH}_3\text{O}_4^\bullet$  takes place in the gas phase, with heat absorption equal to  $110.0 \pm 18.6 \text{ kJ mol}^{-1}$  [17] (without regard for the energy of the possible formation of a hydrogen bond). The exothermic reactions 6 and 7, in which the radicals  $\text{R}^\bullet$  and  $\text{RO}_4^\bullet$  undergo disproportionation, include the isomerization and decomposition of the  $\text{RO}_4^\bullet$  radical. The latter process is likely accompanied by chemiluminescence typical of hydrocarbon oxidation [20]. These reactions regenerate oxygen as  $\text{O}_2$  molecules (including singlet oxygen<sup>4</sup> [20, 27]) and, partially, as  $\text{O}_3$  molecules and yield a carbonyl compound  $\text{R}_{(-2\text{H})}\text{HO}$  (possibly in the triplet excited state [20]). Depending on the decomposition pathway, the other possible products are the alcohol  $\text{ROH}$ , the alkene  $\text{R}_{(-2\text{H})}\text{H}$  (in the case of the oxidation of a saturated hydrocarbon), the ether  $\text{ROR}$ , the alkyl peroxide  $\text{RO}_2\text{R}$ , hydrogen peroxide, and water. It is likely that the isomerization and decomposition of the  $\text{RO}_4^\bullet$  radical via reactions 6 and 7 can take place through the breaking of a C–C bond to yield carbonyl compounds, alcohols, ethers, and organic peroxides containing fewer carbon atoms than the initial hydrocarbon, as in the case of the alkylperoxy radical  $\text{RO}_2^\bullet$  in reaction 3a. At later stages of oxidation and at sufficiently high temperatures, the resulting aldehydes can be further oxidized into respective carboxylic acids. They can also react with molecular oxygen so that a C–H bond in the aldehyde molecule is broken to yield two free radicals ( $\text{HO}_2^\bullet$  and  $\text{R}'_{(-\text{H})}\text{O}$  or  $\text{R}_{(-2\text{H})}\text{O}$ ). This process, like possible ozone decomposition yielding an  $\text{O}^\bullet$  atom or peroxide decomposition with O–O bond breaking, leads to degenerate chain branching [3].

The equations describing the formation rates ( $V$ ) of molecular products at the chain propagation and termination stages of the above reaction scheme, set up using the quasi-steady-state treatment,<sup>5</sup> appear as

$$V_3(\text{RO}_2\text{H}; \text{ROH}) = V_1\alpha k_2 x/f \quad (1)$$

$$= V_1\alpha l x/f_m, \quad (1a)$$

<sup>4</sup> Note that the alkylperoxy radicals  $\text{RO}^\bullet$  are effective quenchers of singlet oxygen  $\text{O}_2(a^1\Delta_g)$  [26].

<sup>5</sup> Deriving the rate equations by this method (which is the most appropriate for processes that involve eight to ten reactions or more and four to six different free radicals and whose curves are based on three to five experimental data points or fewer), we used, for the early stages of the process, a constraint that enabled us to reduce the exponent of the term  $2k_5[\text{R}^\bullet]^2$  in the  $d[\text{R}^\bullet]/dt = 0$  equation to 1 [1, 12]:  $k_6 = \sqrt{2k_5 2k_7}$  [7] and  $V_1 = V_5 + 2V_6 + V_7 = (\sqrt{2k_5}[\text{R}^\bullet] + \sqrt{2k_7}[\text{RO}_4^\bullet])^2$ . Relationships between the reaction rates and the radiation-chemical yields for radiation-induced processes are presented in the concluding section of our earlier paper [1].

$$V_{3a}(\text{R}'_{(-\text{H})}\text{HO}; \text{R}_{(-2\text{H})}\text{HO}) = V_{3b}(\text{R}''\text{OH}; \text{H}_2\text{O}) \\ = V_1\beta k_2 x/f \quad (2)$$

$$= V_1\beta x/f_m, \quad (2a)$$

$$V_5 = V_1^2 2k_5(\alpha l + \beta + x)^2/f^2, \quad (3)$$

$$2V_6 = 2V_1\sqrt{2k_5 V_1}(\alpha l + \beta + x)k_2 x/f^2, \quad (4)$$

$$V_7 = V_1(k_2 x^2)^2/f^2, \quad (5)$$

where  $V_1$  is the initiation rate,  $l = [\text{RH}] \gg [\text{O}_2] = x$ ;  $k_2 = (\alpha l_m + \beta)\sqrt{2k_5 V_1}/x_m^2$  is the rate constant of the addition of the alkyl radical  $\text{R}^\bullet$  to the oxygen molecule (reaction 2) as determined by solving the quadratic equation following from the rate function extremum condition  $\partial V_{3;3a}/\partial x = 0$ ,  $f = k_2 x^2 + (\alpha l + \beta + x)\sqrt{2k_5 V_1}$ , and  $f_m = x^2 + (\alpha l + \beta + x)x_m^2/(\alpha l_m + \beta)$ . Equations (1a) and (2a) were obtained by replacing the rate constant  $k_2$  in Eqs. (1) and (2) with its analytical expression (for reducing the number of unknown parameters to be determined directly).

For  $\alpha l \gg \beta$  ( $V_3 \gg V_{3a}$ ), when the total yield of alkyl hydroperoxides and alcohols having the same number of carbon atoms as the initial compound far exceeds the yield of carbonyl compounds, as in the case of the oxidation of some hydrocarbons, the parameter  $\beta$  in Eq. (1, 1a) can be neglected ( $\beta = 0$ ).

Equations (1) and (2) subject to the constraint  $k_2 x^2 \gg (\alpha l + \beta + x)\sqrt{2k_5 V_1}$  (the descending branch of the peaking curve) can be transformed into Eqs. (6) and (7), respectively, which express simple inverse proportionalities with respect to the initial oxygen concentration  $x$  and allow the parameters  $\alpha$  and  $\beta$  to be tentatively estimated from the experimental product formation rate  $V$  provided that  $V_1$  is known:

$$V_3 = V_1\alpha l/\varphi x, \quad (6)$$

$$V_{3a} = V_1\beta/\varphi x, \quad (7)$$

where  $\varphi = 2$  at the peak point (where  $k_2 x^2 \cong (\alpha l + \beta + x)\sqrt{2k_5 V_1}$ ) and  $\varphi = 1$  for the descending portion of the curve.

The rate ratios for the competing reactions are  $V_3/V_4 = \alpha l/x$  and  $V_{3a}/V_4 = \beta/x$ , and the chain length is  $\nu = (V_3 + V_{3a})/V_1$ . The overall rate of the process is a complicated function of the formation and decay rates of the free radicals  $\text{R}^\bullet$  and  $\text{RO}_4^\bullet$ :  $V(\text{RO}_2\text{H}, \text{R}'_{(-\text{H})}\text{HO}, \text{R}''\text{OH}; \text{ROH}; \text{R}_{(-2\text{H})}\text{HO}, \text{H}_2\text{O}) = V_{1a} + V_3 + V_{3b} - V_4 - V_5 - V_7$ . As distinct from the rates  $V_4$  ( $V_4 \leq V_1$ ),  $V_5$ , and  $V_7$ , the rates  $V_2$ ,  $V_3$ ,  $V_{3a}$ ,  $V_{3b}$ , and  $2V_6$  as a function of the concentration  $x$  have a maximum.

In the alternative kinetic model of oxidation whose chain termination stage involves, in place of  $R^\bullet$ ,  $RO_2^\bullet$  radicals reacting with one another and with  $RO_4^\bullet$  radicals, the relationships between the product formation rates and the oxygen concentration  $x$ , established in the same way, have no maximum:  $V_3 = V_1 k_3 l / (k_4 x + \sqrt{2k_5 V_1})$  and  $V_{3a} = V_1 k_{3a} / (k_4 x + \sqrt{2k_5 V_1})$ . In the kinetic model of oxidation that does not include the competing reaction 4 ( $k_4 = 0$ ) and involves the radicals  $R^\bullet$  and  $RO_2^\bullet$  (the latter instead of  $RO_4^\bullet$ ) in reactions 5–7, the rates  $V_3$  and  $V_{3a}$  obtained in the same way are fractional rational functions of the form of  $a_0 x / (b_0 x + c_0)$ , where  $a_0$ ,  $b_0$ , and  $c_0$  are coefficients having no extremum. For a similar kinetic model in which reactions 3a,b and 4 appearing in the above scheme are missing ( $k_{3a} = k_4 = 0$ , Walling [5], using the quasi-steady-state treatment under the assumption of sufficiently long kinetic chains, when it can be assumed that  $V_2 = V_3$ , without using the substitution  $k_6 = \sqrt{2k_5 2k_7}$  (as distinct from this work), found that  $V_2 = V_3$  is an irrational function of  $x$ :  $ax / \sqrt{bx^2 + cx + d}$  where  $a$ ,  $b$ ,  $c$ , and  $d$  are coefficients. Again, this function does not have a maximum with respect to the concentration of any of the two components.

Thus, of the three kinetic models of oxidation mathematically analyzed above, which involve the radicals  $R^\bullet$  and  $RO_2^\bullet$  in three types of quadratic-law chain termination reactions (reactions 5–7) and are variants of the conventional model [3–8], the last two lead to an oxidation rate versus oxygen concentration curve that emanates from the origin of coordinates, is convex upward, and has an asymptote parallel to the abscissa axis. Such monotonic dependences are observed when the oxygen solubility in the liquid is limited under the given experimental conditions and the oxygen concentration reached is  $[O_2]_{top} \leq x_m$ . Note that  $[O_2]_{top}$  may be below the thermodynamically equilibrium oxygen concentration because of diffusion limitations hampering the establishment of the gas–liquid saturated solution equilibrium under the given experimental conditions (for example, when the gas is bubbled through the liquid) or because the Henry law is violated for the given gas–liquid system under real conditions.

Unlike the conventional model, the above kinetic model of free-radical nonbranched-chain oxidation, which includes the pairs of competing reactions 3–4 and 3a–4 (see the scheme), allows us to describe the nonmonotonic (peaking) dependence of the oxidation rate on the oxygen concentration (Fig. 1). In this oxidation model, as the oxygen concentration in the binary system is increased, oxygen begins to act as an oxida-

tion autoinhibitor or an antioxidant (reactions 4 and 6 lead to inefficient consumption of the free radicals  $RO_2^\bullet$  and  $R^\bullet$  and cause shortening of the kinetic chains). The optimum oxygen concentration  $x_m$ , at which the oxidation rate is the highest, can be calculated using kinetic equations (1a) and (2a) or the corresponding analytical expression for  $k_2$ . In the familiar monograph *Chain Reactions* by N.N. Semenov [28], it is noted that raising the oxygen concentration when it is already sufficient usually slows down the oxidation process by shortening the chains. The existence of the upper (second) ignition limit in oxidation is due to chain termination through triple collisions between an active center of the chain reaction and two oxygen molecules (at sufficiently high oxygen partial pressures). In the gas phase at atmospheric pressure, the number of triple collisions is roughly estimated to be  $10^3$  times smaller than the number of binary collisions (and the probability of a reaction taking place depends on the specificity of the action of the third particle).

Curve 1 in Fig. 1 illustrates the fit between Eq. (1a) at  $\alpha l \gg \beta$  and experimental data for the radiation-induced oxidation of *o*-xylene in the liquid phase at 373 K in the case of 2-methylbenzyl hydroperoxide forming much more rapidly than *o*-tolualdehyde ( $V_3 \gg V_{3a}$  and  $\alpha l \gg \beta$ ) [9]. The limitation of oxygen solubility in *o*-xylene is reached at an oxygen concentration of  $[O_2]_{top} > x_m$ , which corresponds to third experimental point [9]. The oxygen concentration was calculated from the oxygen solubility in liquid xylene at 373 K [29]. The following quantities were used in this mathematical description:  $^{60}Co$   $\gamma$ -radiation dose rate of  $P = 2.18 \text{ Gy s}^{-1}$  [9], total initiation yield of  $G(o\text{-CH}_3\text{C}_6\text{H}_4\dot{\text{C}}\text{H}_2) = 2.6$  particles per 100 eV ( $1.60 \times 10^{-17} \text{ J}$ ) of the energy absorbed by the solution [30];  $V_1 = 4.73 \times 10^{-7} \text{ mol dm}^{-3} \text{ s}^{-1}$ , and  $2k_5 = 1.15 \times 10^{10}$ . The resulting value of the parameter  $\alpha$  is  $(9.0 \pm 1.8) \times 10^{-3}$ ; hence,  $k_2 = (3.2 \pm 0.8) \times 10^5 \text{ dm}^3 \text{ mol}^{-1} \text{ s}^{-1}$ . From data presented in [31], we estimated that  $k_4 = k_3/\alpha = (5.2 \pm 1.2) \times 10^2 \text{ dm}^3 \text{ mol}^{-1} \text{ s}^{-1}$ .

#### ADDITION OF HYDROGEN ATOMS

In the case of hydrogen atom addition to oxygen at moderate temperatures and pressures, when the process does not pass to unsteady-state critical regimes, a number of experimental findings concerning the autoinhibiting effect of an increasing oxygen concentration on hydrogen oxidation in both gas [10, 32, 33] (Fig. 2) and liquid [34] (Fig. 1, curve 2) phases can also be explained in terms of the free-radical addition competition kinetics based on a simplified scheme of nonbranched-chain reactions with only quadratic-law chain termination, without taking into account surface effects [10]. This scheme [35–37] involves the intermediate  $HO_4^\bullet$  [38–40], a low-reactivity hydrotetraoxy rad-

ical,<sup>6</sup> which results from reaction 4 in the above hydrocarbon oxidation scheme with  $R \equiv H$  and  $k_{3a} = 0$  (the enthalpy of reaction 4 in the gas phase without regard for the energy of the possible hydrogen bond in  $HO_4^\bullet$ ,  $\Delta H_{298}^\circ = 110.0 \pm 15.4 \text{ kJ mol}^{-1}$  [17]). The  $HO_4^\bullet$  radical, which does not participate in further chain propagation, shortens the kinetic chains and thus inhibits the chain process. In reaction 5 ( $R \equiv H$ ), when it takes place in the gas phase bulk, the resulting hydrogen molecule has excess energy. Within the treatment used in this study, for this molecule to be stabilized, it must have time to undergo deactivation by a collision with some particle  $M$  capable to take up the excess energy. For the sake of simplicity of kinetic equations, these equations were derived under the assumption that the rate of the bimolecular deactivation of the molecule is well above the rate of the monomolecular decomposition of this molecule, which is the reverse step of reaction 5 [4]. In this case, the rate of the chain formation of hydrogen peroxide (reaction 3) and water (alternative, parenthesized pathway of reaction 3 plus reaction 3b;  $V_3 = V_{3b}$ ) at the chain propagation stage is given by Eq. (1, 1a) with the corresponding analytical expression for  $k_2$  and the rates of the nonchain formation of these products via reactions 6 and 7 at the quadratic-law chain termination stage are given by Eqs. (4) and (5), respectively, with  $\beta = 0$  and  $l = [H_2] \gg [O_2] = x$  in all of these equations:  $V_3(H_2O_2) = V_1 \alpha k_2 x / f = V_1 \alpha k_2 x / f_m$  and  $V_{3, 3b}(H_2O) = 2V_3$ . The ratio of the rates of the competing reactions is  $V_3/V_4 = \alpha/lx$ , and the chain length is  $\nu = V_3/V_1$ . The above equations involve the rate constant of hydrogen atom recombination ( $2k_5$ ), a bimolecular process within the treatment considered. In the case of the pulse radiolysis of ammonia–oxygen gas mixtures at a total pressure of  $10^5 \text{ Pa}$  (including argon) and a temperature of  $349 \text{ K}$ , this constant was calculated to be  $1.6 \times 10^8 \text{ dm}^3 \text{ mol}^{-1} \text{ s}^{-1}$  [33]. (A similar value of this constant for the gas phase was reported in an earlier publication [43].) Furthermore, it was found that the yield of the intermediate  $HO^\bullet$  as a function of the oxygen concentration has a maximum near  $5 \times 10^{-4} \text{ mol dm}^{-3}$  [33].

<sup>6</sup> According to MP2/6-311++G\*\* quantum-chemical calculations carried out by I.V. Trushkov (Faculty of Chemistry, Moscow State University) using the Gaussian 98 program, the cyclic structure  $[\overline{OO-H \cdots OO}]^\bullet$ , closed through a weak hydrogen bond, is energetically more favorable (by  $4.8 \text{ kJ mol}^{-1}$ ) than the open (helical) structure [40] of this radical, for which  $\Delta H_{f, 298}^\circ (HO_4^\bullet) = 122.6 \pm 13.7 \text{ kJ mol}^{-1}$  in the gas phase calculated from data reported in [17]. Further evidence in favor of the cyclic structure of  $HO_4^\bullet$  is that the average lifetime of this radical in water at  $294 \text{ K}$  is  $(3.6 \pm 0.4) \times 10^{-5} \text{ s}$  (evaluated as  $1/k$  for the reaction  $HO_4^\bullet \xrightarrow{k} HO_2^\bullet + O_2$  [39]) 3.9 times longer than the average lifetime of the linear  $HO_4^\bullet$  radical [40, 41] under the same conditions [42].

Curve 2 in Fig. 1 describes, in terms of the overall equation  $V_{3, 7} = V_1 x (\alpha l f_m + x^3) / f_m^2$  for the rates of reactions 3 and 7 of the above scheme with  $R \equiv H$  and  $k_{3a} = 0$  (derived from Eqs. (1a) and (5) with replacement of  $k_2$  in the latter by its analytical expression [44] obtained from Eq. (1), with  $\beta = 0$  in all of the equations), the observed hydrogen peroxide formation rate (minus the rate of the primary formation of hydrogen peroxide after the completion of the reaction in the spurs,  $V_{H_2O_2} = 5.19 \times 10^{-8} \text{ mol dm}^{-3} \text{ s}^{-1}$ ) as a function of the initial concentration of dissolved oxygen in the  $\gamma$ -radiolysis of water saturated with hydrogen ( $7 \times 10^{-4} \text{ mol dm}^{-3}$ ) at a temperature of  $296 \text{ K}$  [34]. In this work, these data were calculated from the slopes of the initial parts of the peroxide-dose curves obtained under  $^{60}\text{Co}$   $\gamma$ -radiation at a dose rate of  $P = 0.67 \text{ Gy s}^{-1}$  and doses of  $D \equiv 22.5\text{--}304.0 \text{ Gy}$  absorbed by the solution. We used the following initial radiation-chemical yields (number of species per  $100 \text{ eV}$  of absorbed energy) of the products of water  $\gamma$ -radiolysis in the solution bulk at pH 4–9 and room temperature (taking into account the relationships  $V = GP$  and  $V_1 = G_H P$ ):  $G_{H_2O_2} = 0.75$  and  $G_H = 0.6$  (initiation yield) [45];  $V_1 = 4.15 \times 10^{-8} \text{ mol dm}^{-3} \text{ s}^{-1}$ ;  $2k_5 = 2.0 \times 10^{10} \text{ dm}^3 \text{ mol}^{-1} \text{ s}^{-1}$  [45]. It can be seen from Fig. 1 that the model taking into account not only the rate  $V_3$  of the chain formation of hydrogen peroxide in the chain propagation reaction 3 (dashed curve; the resulting value of  $\alpha$  is  $0.11 \pm 0.026$ ), but also the rate  $V_7$  of the nonchain formation of the product by the chain termination reaction 7 (curve 2,  $\alpha = (8.5 \pm 2) \times 10^{-2}$ ), becomes the best fit to the experimental data as the oxygen concentration in water increases. However, in order to obtain a more precise kinetic description of the experimental data, it is necessary to take into account the radiation-chemical nature of the process, in particular, oxygen consumption in reactions not included in the hydrogen oxidation scheme [35–37] considered here and the reverse reactions in which the resulting hydrogen peroxide is decomposed by water radiolysis intermediates ( $e_{aq}^-$ ,  $H^\bullet$ , and  $HO^\bullet$ ), among which the hydrated electron plays the major role [45].

Thus, the kinetic model suggested here for the non-catalytic initiated oxidation of hydrocarbons and hydrogen at moderate temperatures and pressures involves, for the first time, the endothermic addition of the  $RO_2^\bullet$  or  $HO_2^\bullet$  radical (1 : 1 adduct), which has an increased energy at the instant it appears, to the oxygen molecule (at sufficiently high oxygen concentrations) with the formation of the radical  $RO_4^\bullet$  or  $HO_4^\bullet$  (1 : 2 adduct) [24, 25]. This reaction competes with chain propagation via the reactive radical  $R^\bullet$  or the H atom (addend). The resulting radical  $RO_4^\bullet$  or  $HO_4^\bullet$  is a low-reactivity species and inhibits the chain process. In this

connection, note that the progressive inhibition of non-branched-chain free-radical processes observed as the concentration of the unsaturated compound (as a source of low-reactivity free radicals) is increased above its optimal value maximizing the process rate may be an element of the self-regulation of natural processes, which brings them back to their stable steady state.

In conclusion, let us note that, in earlier publications [25, 36, 37], we considered a general reaction scheme for the initiated nonbranched-chain addition of free radicals resulting from a saturated compound to an alkene (and its functionalized derivatives), formaldehyde, or oxygen in homogeneous binary liquid systems formed by these components.<sup>7</sup>

#### NOTATION

$k$ —rate constant of a reaction,  $\text{dm}^3 \text{mol}^{-1} \text{s}^{-1}$ ;

$l, x$ —initial molar concentrations of the hydrocarbon and oxygen dissolved in this hydrocarbon, respectively,  $\text{mol dm}^{-3}$ ;

$l_m, x_m$ —values of  $l$  and  $x$  at the point of maximum of the functionality;

$V$ —reaction rate,  $\text{mol dm}^{-3} \text{s}^{-1}$ ;

$\alpha = k_3/k_4, \beta = k_{3a}/k_4$ —ratios of the rate constants of competing (parallel) reactions; the dimension of the latter is  $\text{mol dm}^{-3}$ .

#### SUBSCRIPTS

1, 2, ..., 7—reaction number in the process scheme;

$m$ —maximum value.

#### REFERENCES

1. Silaev, M.M., Simulation of the Nonbranched-Chain Addition of Saturated Free Radicals to Alkenes and Their Derivatives Yielding 1 : 1 Adducts, *Teor. Osn. Khim. Tekhnol.*, 2007, vol. 41, no. 3, p. 289 [*Theor. Found. Chem. Eng.* (Engl. Transl.), vol. 41, no. 3, p. 273].
2. Silaev, M.M., Simulation of Nonbranched Chain Processes for Producing 1,2-Alkanediols in Alcohol-Formaldehyde Systems, *Teor. Osn. Khim. Tekhnol.*, 2007, vol. 41, no. 4, p. 379 [*Theor. Found. Chem. Eng.* (Engl. Transl.), vol. 41, no. 4, p. 357].
3. Emanuel, N.M., Denisov, E.T., and Maizus, Z.K., *Tsepnye reaktsii okisleniya uglevodorodov v zhidkoi faze* (Chain Oxidation of Hydrocarbons in the Liquid Phase), Moscow: Nauka, 1965.
4. Benson, S.W., *Thermochemical Kinetics. Methods for the Estimation of Thermochemical Data and Rate Parameters*, New York: Wiley, 1976, 2nd ed.

5. Walling, C., *Free Radicals in Solution*, New York: Wiley, 1957.
6. Shtern, V.Ya., *Mekhanizm okisleniya uglevodorodov v gazovoi faze* (Mechanism of the Gas-Phase Oxidation of Hydrocarbons), Moscow: Akad. Nauk SSSR, 1960.
7. Bateman, L., Olefin Oxidation, *Quart. Rev.*, 1954, vol. 8, no. 2, p. 147.
8. Bäckström, H.L.J., Der Kettenmechanismus bei der Autoxydation von Aldehyden, *Z. Phys. Chem. B*, 1934, vol. 25, no. 1, p. 99.
9. Aliev, A.A. and Saraeva, V.V., Isomerization of Peroxy Radicals Resulting from the Radiation-Induced Oxidation of *o*-Xylene, *Vestn. Mosk. Univ., Ser. 2: Khim.*, 1983, vol. 24, no. 4, p. 371.
10. Badin, E.J., The Reaction between Atomic Hydrogen and Molecular Oxygen at Low Pressures. Surface Effects, *J. Am. Chem. Soc.*, 1948, vol. 70, no. 11, p. 3651.
11. Silaev, M.M. and Bugaenko, L.T., Mathematical Simulation of the Kinetics of Radiation Induced Hydroxyalkylation of Aliphatic Saturated Alcohols, *Radiat. Phys. Chem.*, 1992, vol. 40, no. 1, p. 1.
12. Silaev, M.M. and Bugaenko, L.T., The Kinetics of  $\alpha$ -Hydroxyalkyl Radical Addition to 2-Propen-1-ol and Formaldehyde, *Kinet. Katal.*, 1994, vol. 35, no. 4, p. 509 [*Kinet. Catal.* (Engl. Transl.), vol. 35, no. 4, p. 463].
13. Gurvich, L.V., Karachevtsev, G.V., Kondrat'ev, V.N., et al., *Energii razryva khimicheskikh svyazei. Potentsialy ionizatsii i srodstvo k elektronu* (Bond Dissociation Energies, Ionization Potentials, and Electron Affinity), Kondrat'ev, V.N., Ed., Moscow: Nauka, 1974.
14. Orlov, Yu.D., Lebedev, Yu.A., and Saifullin, I.Sh., *Termokhimiya organicheskikh svobodnykh radikalov* (Thermochemistry of Organic Free Radicals), Kutepov, A.M., Ed., Moscow: Nauka, 2001.
15. Pedley, J.B., Naylor, R.D., and Kirby, S.P., *Thermochemical Data of Organic Compounds*, London: Chapman & Hall, 1986, 2nd ed.
16. Buchachenko, A.L., *Kompleksy radikalov i molekulyarnogo kisloroda s organicheskimi molekulami* (Complexes of Radicals and Dioxygen with Organic Molecules), Beletskaya, I.P., Ed., Moscow: Nauka, 1984.
17. Francisco, J.S. and Williams, I.H., The Thermochemistry of Polyoxides and Polyoxy Radicals, *Int. J. Chem. Kinet.*, 1988, vol. 20, no. 6, p. 455.
18. Kokorev, V.N., Vyshinskii, N.N., Maslennikov, V.P., et al., Electronic Structure and Chemical Reactions of Peroxides: I. MINDO/3 Calculation of the Geometry and Enthalpy of Formation of the Ground States of Organic and Organoelement Peroxides, *Zh. Strukt. Khim.*, 1981, vol. 22, no. 4, p. 9.
19. Dmitruk, A.F., Lobanov, V.V., and Kholoimova, L.I., Role of Tetroxide Conformation in the Mechanism of Peroxy Radical Recombination, *Teor. Eksp. Khim.*, 1986, vol. 22, no. 3, p. 363.
20. Belyakov, V.A., Vasil'ev, R.F., Ivanova, N.M., et al., Electronic Model of the Excitation of Chemiluminescence in the Oxidation of Organic Compounds, *Izv. Akad. Nauk SSSR, Ser. Fiz.*, 1987, vol. 51, no. 3, p. 540.
21. Ase, P., Bock, W., and Snelson, A., Alkylperoxy and Alkyl Radicals. 1. Infrared Spectra of  $\text{CH}_3\text{O}_2$  and  $\text{CH}_3\text{O}_4\text{CH}_3$  and the Ultraviolet Photolysis of  $\text{CH}_3\text{O}_2$  in

<sup>7</sup> In one of these publications [36], the parameter  $\beta$  is missing in the numerator of the right-hand side of the equation for the reaction rate  $2V_6$ , so this equation is actually identical to Eq. (4) appearing in this article.

- Argon + Oxygen Matrices, *J. Phys. Chem.*, 1986, vol. 90, no. 10, p. 2099.
22. Pimentel, G.C. and McClellan, A.L., *The Hydrogen Bond*, Pauling, L., Ed., San Francisco: Freeman, 1960, p. 200.
  23. Russell, G.A., Deuterium-Isotope Effects in the Autooxidation of Alkyl Hydrocarbons: Mechanism of the Interaction of Peroxy Radicals, *J. Am. Chem. Soc.*, 1957, vol. 79, no. 14, p. 3871.
  24. Silaev, M.M., The Competition Kinetics of Nonbranched Chain Processes of Free-Radical Addition to Double Bonds of Molecules with the Formation of 1 : 1 Adducts and the Inhibition by the Substrate, *Oxid. Commun.*, 1999, vol. 22, no. 2, p. 159.
  25. Silaev, M.M., The Competition Kinetics of Radical-Chain Addition, *Zh. Fiz. Khim.*, 1999, vol. 73, no. 7, p. 1180 [*Russ. J. Phys. Chem.* (Engl. Transl.), vol. 73, no. 7, p. 1050].
  26. Darmanyan, A.P., Gregory, D.D., Guo, Y., et al., Quenching of Singlet Oxygen by Oxygen- and Sulfur-Centered Radicals: Evidence for Energy Transfer to Peroxy Radicals in Solution, *J. Am. Chem. Soc.*, 1998, vol. 120, no. 2, p. 396.
  27. Kanofsky, J.R., Singlet Oxygen Production from the Reactions of Alkylperoxy Radicals. Evidence from 1268-nm Chemiluminescence, *J. Org. Chem.*, 1986, vol. 51, no. 17, p. 3386.
  28. Semenov, N.N., *Tsepnye reaktsii* (Chain Reactions), Moscow: Nauka, 1986, pp. 173, 148.
  29. Reznikovskii, M., Tarasova, Z., and Dogadkin, B., Oxygen Solubility in Some Organic Liquids, *Zh. Obshch. Khim.*, 1950, vol. 20, no. 1, p. 63.
  30. Saraeva, V.V., *Okislenie organicheskikh soedinenii pod deistviem ioniziruyushchikh izluchenii* (Ionizing Radiation-Induced Oxidation of Organic Compounds), Moscow: Mosk. Gos. Univ., 1991, p.137.
  31. Howard, J.A. and Ingold, K.U., Absolute Rate Constants for Hydrocarbon Autooxidation. VI. Alkyl Aromatic and Olefinic Hydrocarbons, *Can. J. Chem.*, 1967, vol. 45, no. 8, p. 793.
  32. Smith, H.A. and Napravnik, A., The Photochemical Oxidation of Hydrogen, *J. Am. Chem. Soc.*, 1940, vol. 62, no. 1, p. 385.
  33. Pagsberg, P.B., Eriksen, J., and Christensen, H.C., Pulse Radiolysis of Gaseous Ammonia-Oxygen Mixtures, *J. Phys. Chem.*, 1979, vol. 83, no. 5, p. 582.
  34. Barr, N.F. and Allen, A.O., Hydrogen Atoms in the Radiolysis of Water, *J. Phys. Chem.*, 1959, vol. 63, no. 6, p. 928.
  35. Silaev, M.M., Competitive Mechanism of the Nonbranched Radical Chain Oxidation of Hydrogen Involving the Free Cyclohydrotetraoxyl Radical  $[\text{OO}\cdots\text{H}\cdots\text{OO}]^*$ , Which Inhibits the Chain Process, *Khim. Vys. Energ.*, 2003, vol. 37, no. 1, p. 27 [*High Energy Chem.* (Engl. Transl.), vol. 37, no. 1, p. 24].
  36. Silaev, M.M., Competition Kinetics of Nonbranched Chain Processes of Free Radical Addition to the C=C, C=O, and O=O Double Bonds of Molecules, *Neftekhimiya*, 2003, vol. 43, no. 4, p. 302 [*Pet. Chem.* (Engl. Transl.), vol. 43, no. 4, p. 258].
  37. Silaev, M.M., Low-Reactive Free Radicals Inhibiting Nonbranched Chain Processes of Addition, *Biofizika*, 2005, vol. 50, no. 4, p. 585 [*Biophysics* (Engl. Transl.), vol. 20, no. 4, p. 511].
  38. Bahnemann, D. and Hart, E.J., Rate Constants of the Reaction of the Hydrated Electron and Hydroxyl Radical with Ozone in Aqueous Solution, *J. Phys. Chem.*, 1982, vol. 86, no. 2, p. 252.
  39. Staehelin, J., Bühler, R.E., and Hoigné, J., Ozone Decomposition in Water Studied by Pulse Radiolysis. 2. OH and HO<sub>4</sub> As Chain Intermediates, *J. Phys. Chem.*, 1984, vol. 88, no. 24, p. 5999.
  40. McKay, D.J. and Wright, J.S., How Long Can You Make an Oxygen Chain?, *J. Am. Chem. Soc.*, 1998, vol. 120, no. 5, p. 1003.
  41. Cacace, F., de Petris, G., Pepi, F., and Troiani, A., Experimental Detection of Hydrogen Trioxide, *Science*, 1999, vol. 285, no. 5424, p. 81.
  42. Bühler, R.E., Staehelin, J., and Hoigné, J., Ozone Decomposition in Water Studied by Pulse Radiolysis. 1. HO<sub>2</sub>/O<sub>2</sub><sup>-</sup> and HO<sub>3</sub>/O<sub>3</sub><sup>-</sup> As Intermediates, *J. Phys. Chem.*, 1984, vol. 88, no. 12, p. 2560.
  43. Boyd, A.W., Willis, C., and Miller, O.A., A Re-examination of the Yields in the High Dose Rate Radiolysis of Gaseous Ammonia, *Can. J. Chem.*, 1971, vol. 49, no. 13, p. 2283.
  44. Silaev, M.M., Competitive Mechanism of Substrate-Inhibited Radical Chain Addition to Double Bond, *Neftekhimiya*, 2000, vol. 40, no. 1, p. 33 [*Pet. Chem.* (Engl. Transl.), vol. 40, no. 1, p. 29].
  45. Pikaev, A.K., *Sovremennaya radiatsionnaya khimiya. Radioliz gazov i zhidkosti* (Modern Radiation Chemistry. Radiolysis of Gases and Liquids), Moscow: Nauka, 1986.